Journal of
Synchrotron Radiation

ISSN 0909-0495

Received 20 September 2006
Accepted 29 January 2007

Diffraction-based automated crystal centering

Jinhu Song,[a,b] Deepa Mathew,[a,b] Sandhya A. Jacob,[a,b] Laura Corbett,[a,b] Penjit Moorhead[a,b] and S. Michael Soltis[a,b]*

[a]Stanford Synchrotron Radiation Laboratory, 2575 Sand Hill Road, Menlo Park, CA 94025, USA, and [b]Stanford Linear Accelerator Center, 2575 Sand Hill Road, Menlo Park, CA 94025, USA. E-mail: soltis@slac.stanford.edu

A fully automated procedure for detecting and centering protein crystals in the X-ray beam of a macromolecular crystallography beamline has been developed. A cryo-loop centering routine that analyzes video images with an edge detection algorithm is first used to determine the dimensions of the loop holding the sample; then low-dose X-rays are used to record diffraction images in a grid over the edge and face plane of the loop. A three-dimensional profile of the crystal based on the number of diffraction spots in each image is constructed. The derived center of mass is then used to align the crystal to the X-ray beam. Typical samples can be accurately aligned in ~2–3 min. Because the procedure is based on the number of 'good' spots as determined by the program *Spotfinder*, the best diffracting part of the crystal is aligned to the X-ray beam.

© 2007 International Union of Crystallography
Printed in Singapore – all rights reserved

Keywords: crystal alignment and centering; beamline automation.

1. Introduction

Structure-based biology is entering a new phase with the automation and optimization of X-ray crystallography methods. High-throughput structural genomics and drug discovery pipelines are being optimized and automated from the initial target selection to final structure determination (Abola *et al.*, 2000). One of the key steps is the collection of X-ray diffraction data and when fully automated will enable unattended and efficient data collection experiments (Kuhn & Soltis, 2001). Automating all aspects of the diffraction experiment, including mounting and centering the crystal in the X-ray beam, would increase the efficacy and success of high-throughput beamline experiments in general (Leslie *et al.*, 2002).

The recent development of robotic systems to mount protein samples on synchrotron beamlines has significantly increased the efficiency of data collection. For example, the system developed at Stanford Synchrotron Radiation Laboratory (SSRL) can mount up to 288 samples automatically and can screen each one for diffraction quality in less than 15 h without human intervention (Cohen *et al.*, 2002). Many robotic facilities have recently been developed for macromolecular crystallography experiments (Muchmore *et al.*, 2000; Karain *et al.*, 2002; Shu *et al.*, 2003; Snell *et al.*, 2004; Pohl *et al.*, 2004; Ohana *et al.*, 2004; Ueno *et al.*, 2004; Cipriani *et al.*, 2006), and a current listing of installations can be found on the Robosync website: http://smb.slac.stanford.edu/facilities/hardware/SAM/robosync/.

Cryo-loop centering routines are often employed for aligning the loop containing the sample crystal to the X-ray beam, enabling automated crystal screening. By utilizing a beam size that is the same size or larger than the size of the loop, test images of crystals can be readily obtained. Although hundreds of samples can be automatically screened for diffraction quality in this manner, a conventional data collection experiment requires accurate alignment of the crystal to the X-ray beam. Several automated methods for detecting or centering crystals have recently been developed (Muchmore *et al.*, 2000; Karain *et al.*, 2002; Roth *et al.*, 2002; Andrey *et al.*, 2004; Lavault *et al.*, 2006; Pothineni *et al.*, 2006). However, these methods use visible light and depend heavily on crystal contrast. Inadequate lighting conditions or the inability to distinguish crystal edges from ice, solvent or the loop can sometimes hinder the determination of the crystal position. A method for aligning samples using UV laser-excited fluorescence was recently described which requires the use of non-fluorescent loops (Vernede *et al.*, 2006). Although the method also requires the use of a high-powered laser, the exposure time is short and thus the alignment of the sample can be very rapid.

In this paper we describe a fully automated crystal diffraction analysis procedure to center the crystal to the X-ray beam. This method only requires visualization of the loop and does not require visualization of the crystal or any special set-up of the experimental equipment. Because the analysis is based on diffraction, the best diffracting part of the crystal is aligned to the beam.

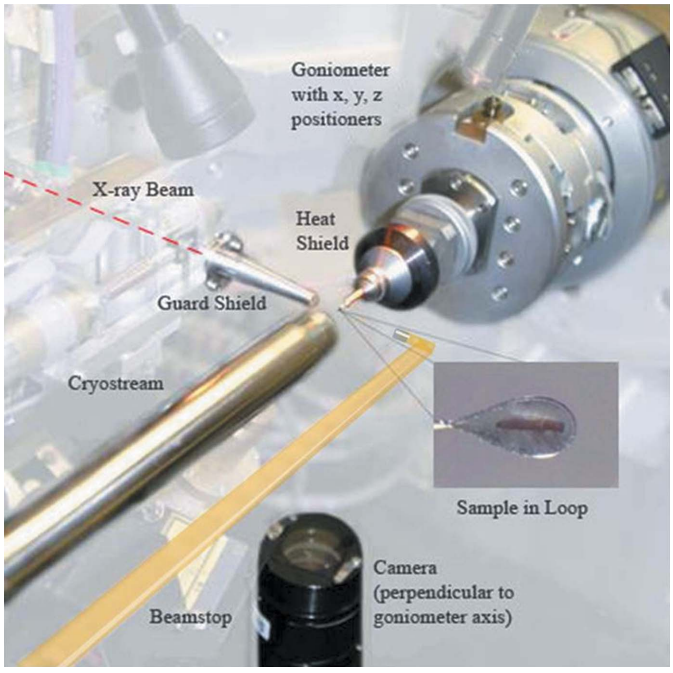

Figure 1
Standard experimental set-up on the SSRL protein crystallography beamlines.

2. Crystal centering overview

The sample centering procedure is carried out in a two-step process: first, the cryo-loop is centered using image analysis and then the crystal is centered on the X-ray beam using a low-dose X-ray diffraction analysis. The center of mass of the crystal is determined from the number of recorded diffraction spots in a three-dimensional grid search of the loop volume. This method is versatile and does not depend on specific crystal cryo-cooling conditions, visibility, color or shape.

3. Instrumentation

Fig. 1 shows the standard camera set-up on the SSRL crystallography beamlines. The crystalline sample is suspended in a fine nylon loop which is attached to a standard Hampton micro-tube and magnetic pin. The pin is held onto the goniometer by a magnet. The sample is aligned to the X-ray beam using motorized x, y and z translations mounted on the φ rotation axis. The sample is held near 100 K using a cryogenic gas stream that is coaxial with the φ axis. A camera that views the sample from below provides real-time video of the sample position. The camera viewing the sample is equipped with an automated zoom feature allowing for a magnification range of 2–20 µm pixel^{-1} and a corresponding field of view range of 0.7–7 mm.

4. Automated loop centering

A script was developed at SSRL to align the sample loop to the X-ray beam based on image analysis (van den Bedem *et al.*, 2003; Miller *et al.*, 2004). This technique is extremely robust and allows for automated screening of variable-sized crystals as long as the crystal or part of the crystal is within the loop and the beam size roughly matches or is larger than the size of the loop. During loop centering, a series of video images is collected while the loop is rotated around the φ rotation axis; edge detection techniques are then used to determine the face and edge of the loop and ultimately the three-dimensional volume of the loop and crystal together. The dimensions and orientation of the loop and sample are obtained in ~30 s, and the resulting volume is used for the diffraction grid search.

5. Diffraction grid search

Crystal centering is carried out by collecting diffraction images spanning the loop volume. First, the edge view of the loop is divided into a 3 × 3 grid based on the horizontal length and vertical height of the loop as determined by the automated loop centering routine (Fig. 2*a*). The overall search time is significantly reduced by evaluating the edge first because it is typically smaller in area than the face of the loop (Fig. 2*b*). The X-ray beam size is set to the size of each grid component and can differ in the horizontal and vertical directions (Fig. 2*a*). Larger grids (*i.e.* 4 × 4) are used when the grid size is limited by the maximum beam size available at a particular beamline.

Each grid component of the loop is sequentially positioned on the X-ray beam for a low-dose exposure (Fig. 3). If diffraction spots are recorded in only one or two components of the grid, the component or components indicating diffraction are used to define a new smaller 3 × 3 grid. If diffraction is recorded for three components in a column or row, a calculation is carried out using the number of diffraction spots to estimate the weighted center of mass and the effective length of the crystal.

The effective crystal length is estimated by summing the number of spots in the three components and dividing by 3×

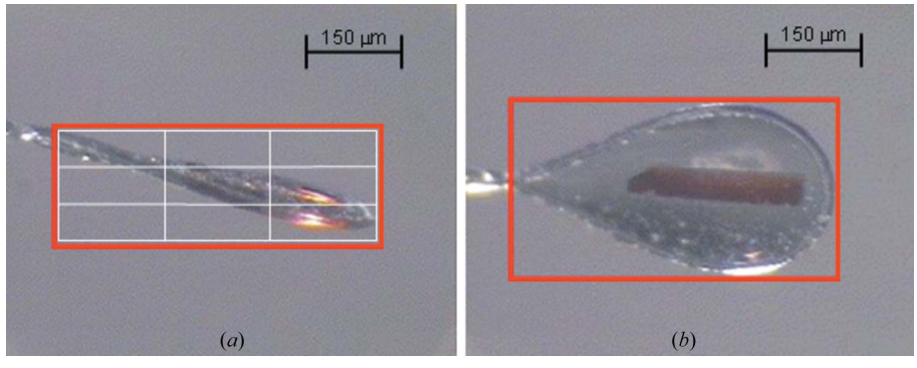

Figure 2
(*a*) Edge view and (*b*) face view (90° from the face view) of a loop containing a protein crystal. The box shown in red indicates the horizontal length and vertical height of the loop and crystal as determined using the loop centering routine. The initial 3 × 3 search grid for the loop edge is shown in white.

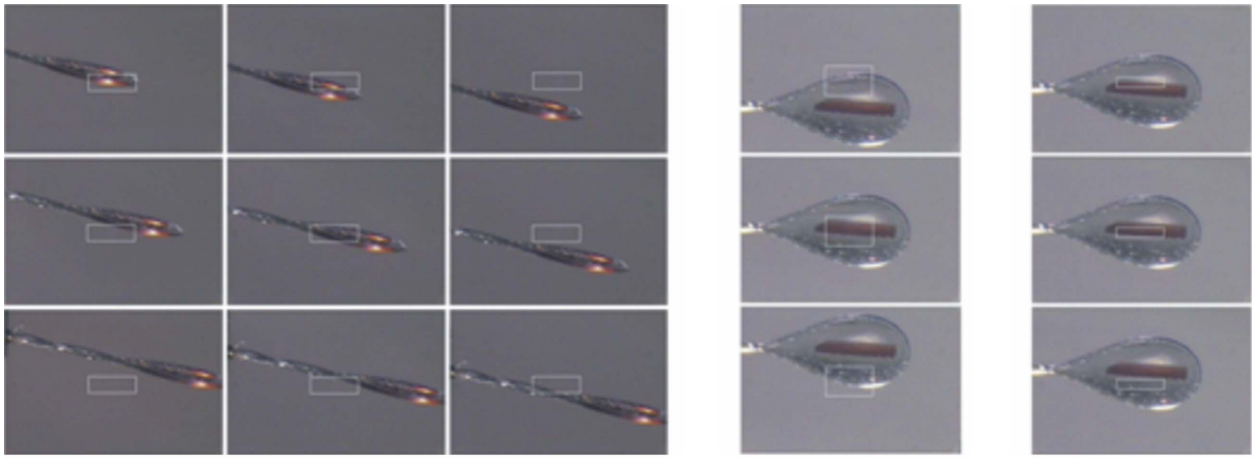

(*a*) (*b*) (*c*)

Figure 3
View of loop and sample in the direction of the X-ray beam. The white box indicates the position and size of the beam. (*a*) The initial 3 × 3 diffraction grid search spanning the edge of the loop. The sample is translated sequentially for each diffraction image. (*b*) An initial 1 × 3 grid on the face of the loop, 90° from the edge view. (*c*) A smaller 1 × 3 grid in the vertical direction, centering in on the crystal. Note that the horizontal width of the beam in (*b*) and (*c*), which is derived from the previous grid search of the loop edge, is smaller than the crystal length and is not centered on the crystal in this case owing to significantly lower quality and disproportionate diffraction from the ends of the crystal.

the number of spots recorded in the central component. This method gives rise to effective lengths that are sometimes smaller than the actual crystal size when the crystal diffracts weakly on the ends of the crystal as shown in Figs. 3(*b*) and 3(*c*).

The search is considered complete when the estimated length is more than 60% of the total length of the search grid. However, if the estimated length is less than 60% of the overall grid size, a new smaller grid is constructed based on the estimated center and length of the crystal. This process is repeated until enough data are recorded to meet the above criteria or when the minimum beam size is reached, at which time a final center of mass is calculated based on the available data.

Once the center of mass is determined for the loop edge, the sample is rotated 90° to the face, and a 1 × 3 grid search is carried out (Fig. 3*b*). The horizontal beam size is set to the horizontal width of the crystal as determined in the previous step. An example of a smaller grid search is shown in Fig. 3(*c*), where a smaller grid and vertical step size are used to center in on the crystal.

Once determined in three dimensions, the center of mass of the crystal is moved to the X-ray beam; the crystal is positioned to yield the best diffraction for data collection.

6. Determining the exposure time for image analysis

A key element of the auto-alignment procedure is the use of low-intensity exposures which minimizes radiation damage to the crystal, yet yields 100–200 diffraction spots per image for image analysis. Based on the beamline characteristics, the initial exposure time is set to record ∼150 diffraction spots [as determined from the program *Spotfinder* (Zhang *et al.*, 2006)] for a typical diffracting crystal. On SSRL beamlines 9-1 and 11-1 the initial exposure time is typically set to 0.5 s. When there is an X-ray exposure limitation with the experimental hardware (typically less than 1 s), aluminium filters are used to attenuate the X-ray beam.

If more than 200 diffraction spots are recorded, the dose is proportionally reduced to produce approximately 175 spots for subsequent grid searches. If the maximum number of spots is less than 100, the dose is increased to achieve ∼175 spots and the grid search is repeated. If no diffraction spots are found in the images, the initial exposure time is incremented, and the grid procedure is repeated. This process continues until enough diffraction spots are recorded in at least one component of the grid or until the pre-set maximum exposure time is exceeded.

When subsequent grids of reduced size are used, the exposure time is also adjusted by the ratio of the beam sizes to yield approximately the same number of diffraction spots per image.

7. Image analysis

Another key step in the crystal centering routine is the analysis of the diffraction images. In a series of preliminary experiments, it was determined that the average $I/\sigma(I)$ for each integrated diffraction image could be used to determine the crystal center of mass. For this analysis, *MOSFLM* (Leslie, 1992) was used to determine the average $I/\sigma(I)$ values for each component diffraction pattern. However, the overall time required for the analysis was relatively long.

An alternative parameter was investigated for estimating the center of mass from the diffraction images; the number of 'good' diffraction spots as determined using the program *Spotfinder* was found to be essentially equivalent to measuring $I/\sigma(I)$ for the purpose of crystal alignment. *Spotfinder* distinguishes 'good' spots from 'bad' spots using spot shape analysis, ice ring detection *etc. Spotfinder* is also configured to exclude

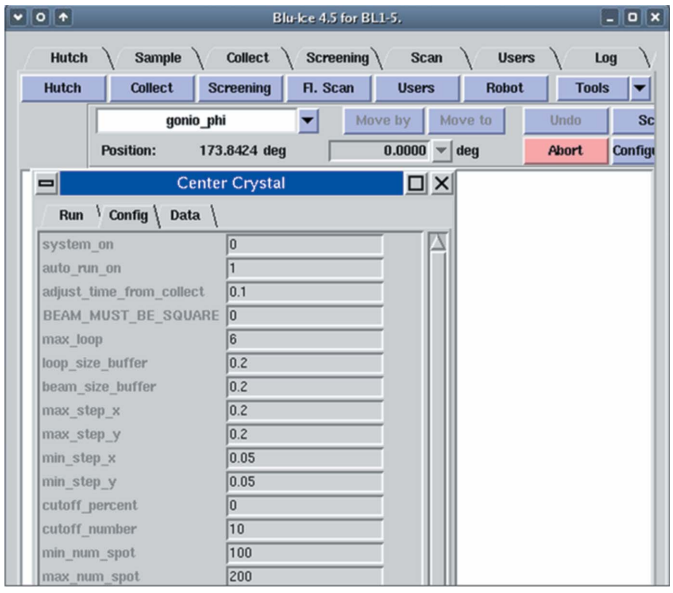

Figure 4
New crystal centering window in the 'Staff' tab of *Blu-Ice*. The 'Config' tab is used to set beamline-specific parameters. The interface also includes a run log and a screen for debugging new beamline implementations.

spots with multiple peaks. The default parameters are normally set to reject low-intensity peaks and peaks outside a limited resolution range. However, for this analysis the minimum intensity pixel threshold was lowered from 1000 to 100 counts and the resolution limitations were removed.

Images are processed as soon as they are generated and run in parallel on multiple CPUs, taking an average of 6 s each to complete.

8. *Blu-Ice* interface

A new tool was implemented for crystal centering in the 'Staff' tab of the beamline control graphical user interface (GUI), *Blu-Ice* (McPhillips *et al.*, 2002)[1]. The 'Config' tab allows staff to set the appropriate parameters for the crystal centering routine (Fig. 4). These parameters are typically beamline specific. Two additional tabs are available that display current values for debugging and a run log of the centering process. For normal operation, a new 'Align Crystal' button has been added to the data collection tab in the *Blu-Ice* GUI. This feature can be used when the crystal cannot be centered visually or when optimal diffraction quality is desired for data collection.

9. Test conditions

9.1. Crystals

Different types of crystals were used to test the auto-crystal alignment program including lysozyme, sperm whale myoglobin and a variety of proteins from *Thermotoga maritima* supplied by the Joint Center for Structural Genomics (JCSG). Approximately 50 samples were mounted in Hampton Research cryo-loops with varying diameters of 0.05, 0.1, 0.2, 0.3, 0.4 and 0.7 mm. Crystals were selected to cover a range of factors including size, shape and orientation. Diffraction limits of the samples ranged from 1.3 to 3 Å.

9.2. Beamline parameters

SSRL beamlines 9-2 and 11-1 were used to test the alignment software, each supplying a dose of $\sim 10^{11}$ photons s^{-1} through at 200 µm × 200 µm square aperture at 12 keV. The software was configured to use the standard beam size ranges on these beamlines (30–300 µm). Smaller beam sizes (tested to 20 µm) could be used with proportionally longer exposure times. Data were collected using an X-ray energy of 12 keV and a sample-to-detector distance in the range 200–400 mm.

10. Results

The centering routine was used to successfully align crystals ranging in size from 0.7 to 0.03 mm on edge to the center of the X-ray beam. Reproducibility was within 10% of the crystal size. For samples where the loop was no more than a factor of two larger than the crystal, the entire alignment process took typically 2–3 min using ~20 low-dose exposures to the crystal which was the equivalent of one or two normal data-collection exposures that would achieve the diffraction resolution limit. Samples with loops mounted at an angle of 45° with respect to the φ rotation axis are typically centered in 4–5 min. For very small crystals (<50 µm) in large loops (~0.5 mm) the process could run up to 10 min. Although the routine runs longer in the latter cases, the actual exposure to the sample is still of the order of one or two normal exposures. The smallest crystal that can be aligned is generally the size of the smallest beam available.

While testing the alignment routine, two important observations were made: (i) for any given beam profile, crystals were aligned to the hottest part of the X-ray beam; (ii) the best diffracting part of the crystal was aligned to the beam. These observations are consistent with the fact that the diffraction analysis is based on the diffraction strength of the crystal and the number of 'good' spots as determined from *Spotfinder*. The algorithm utilized could also be used to accurately position the collimator that defines the position and size of the X-ray beam with respect to the φ rotation axis. A prototype routine to automate this alignment process is being tested. Current reproducibility of the alignment procedure using a very well defined 50 µm cube crystal is ~3 µm. Moreover, an estimate of the crystal size could also be made based on the diffraction analysis and in practice could be used to set an optimal beam size for data collection. A separate study was carried out where the average $I/\sigma(I)$ was calculated from diffraction images of crystals in the same orientation but with varying beam sizes. Typically, $I/\sigma(I)$ was found to be optimal when the beam size was ~20% larger than the size deter-

[1] To obtain a copy of the *Blu-Ice* source code for evaluation or installation, visit http://smb.slac.stanford.edu/public/research/developments/blu-ice/.

mined using the crystal centering routine, due in part to the convergence of the X-ray beam on beamlines 9-2 and 11-1. The current crystal centering routine adjusts the final beam size to the calculated crystal size plus a fixed percentage that can be selected for each beamline in the *Blu-Ice* 'Crystal Centering Config' tab.

11. Conclusions

A robust routine for automatically aligning crystals to the X-ray beam using low-dose X-ray diffraction data has been successfully implemented in the *Blu-Ice*/*DCS* macromolecular crystallography beamline control software package. This routine optimally aligns samples without visual bias. The best diffracting part of the crystal is aligned to the most intense part of the X-ray beam and the optimal beam size is also estimated for data collection. Furthermore, a prototype routine is being developed to automatically align the X-ray beam collimator to the center of the goniometer φ rotation axis. These developments have made a significant contribution towards the goal of a complete automated data collection pipeline.

Special thanks to I. Mathews and JCSG for providing crystals, Brendon Soltis for preparing figures and Aina Cohen for reviewing the paper. This research was carried out at the Stanford Synchrotron Radiation Laboratory, a national user facility operated by Stanford University on behalf of the US Department of Energy, Office of Basic Energy Sciences. The SSRL Structural Molecular Biology Program is supported by the Department of Energy, Office of Biological and Environmental Research, and by the National Institutes of Health, National Center for Research Resources, Biomedical Technology Program, and the National Institute of General Medical Sciences.

References

Abola, E., Kuhn, P., Earnest, T. & Stevens, R. C. (2000). *Nat. Struct. Biol. Suppl.* **7**, 973–977.

Andrey, P., Lavault, B., Cipriani, F. & Maurin, Y. (2004). *J. Appl. Cryst.* **37**, 265–269.

Bedem, H. van den, Miller, M. D. & Wolf, G. (2003). *Synchrotron Rad. News*, **16**, 15–19.

Cipriani, F. *et al.* (2006). *Acta Cryst.* D**62**, 1251–1259.

Cohen, A. E., Ellis, P. J., Miller, M. D., Deacon, A. M. & Phizackerley, R. P. (2002). *J. Appl. Cryst.* **35**, 720–726.

Karain, W. I., Bourenkov, G. P., Blume, H. & Bartunik, H. D. (2002). *Acta Cryst.* D**58**, 1519–1522.

Kuhn, P. & Soltis, S. M. (2001). *Nucl. Instrum. Methods Phys. Res. A*, **467**, 1363–1366.

Lavault, B., Ravellia, R. B. G. & Cipriania, F. (2006). *Acta Cryst.* D**62**, 1348–1357.

Leslie, A. G. W. (1992). *Joint CCP4 + ESF-EAMCB Newsletter on Protein Crystallography*, No. 26. (MOSFLM Users Guide, Version 6.2.6, http://www.mrc-lmb.cam.ac.uk/harry/mosflm/mosflm_user_guide.html).

Leslie, A. G. W., Powell, H. R., Winter, G., Svensson, O., Spruce, D., McSweeney, S., Love, D., Kinder, S., Duke, E. & Nave. C. (2002). *Acta Cryst.* D**58**, 1924–1928.

McPhillips, T. M, McPhillips, S. E., Chiu, H.-J., Cohen, A. E., Deacon, A. M., Ellis, A. M., Garman, E., Gonzalez, A., Sauter, N. K., Phizackerley, R. P., Soltis S. M. & Kuhn, P. (2002). *J. Synchrotron Rad.* **9**, 401–406.

Miller, M. D., Brinen, L. S., Cohen, A., Deacon, A. M., Ellis, P., McPhillips, S. E., McPhillips, T. M., Phizackerley, R. P., Soltis, S. M., van den Bedem, H., Wolf, G., Xu, Q. & Zhang, Z. (2004). *Eighth International Conference on Synchrotron Radiation Instrumentation (SRI2003), AIP Conference Proceedings 705*, San Francisco, CA, USA, August 2003, pp. 1233–1236. Melville, NY: American Institute of Physics.

Muchmore, S. W., Olson, J., Jones, R., Pan, J., Blum, M., Greer, J., Merrick, S. M., Magdalinos, P. & Nienaber, V. L. (2000). *Structure*, **8**, R243–R246.

Ohana, J., Jacquamet, L., Joly, J., Bertoni, A., Taunier, P., Michel, L., Charrault, P., Pirocchi, M., Carpentier, P., Borel, F., Kahn, R. & Ferrer, J.-L. (2004). *J. Appl. Cryst.* **37**, 72–77.

Pohl, E., Ristau, U., Gehrmann, T., Jahn, D., Robrahn, B., Malthan, D., Dobler, H. & Hermes, C. (2004). *J. Synchrotron Rad.* **11**, 372–377.

Pothineni, S. B., Strutz, T. & Lamzin, V. S. (2006). *Acta Cryst.* D**62**, 1358–1368.

Roth, M., Carpentier, P., Kaikati, O., Joly, J., Charrault, P., Pirocchi, M., Kahn, R., Fanchon, E., Jacquamet, L., Borel, F., Bertoni, A., Israel-Gouy, P. & Ferrer, J.-L. (2002). *Acta Cryst.* D**58**, 805–814.

Shu, D., Toellner, T. S., Alp, E. E., Maser, J., Mancini, D., Lai, B., McNulty, I., Joachimiak, A., Lee, P., Lee, W.-K., Cai, Z., Lee, S.-H., Han, Y., Preissner, C., Ginell, S., Alkire, R. & Schuessler, R. (2003). *2nd International Workshop on Mechanical Engineering Design of Synchrotron Radiation Equipment and Instrumentation (MEDSI02)*, 5–6 September 2002, pp. 214–222, Advanced Photon Source, Argonne National Laboratory, Argonne, IL, USA.

Snell, G., Cork, C., Nordmeyer, R., Cornell, E., Meigs, G., Yegian, D., Jaklevic, J., Jin, J., Stevens, R. C. & Earnest, T. (2004). *Structure*, **12**, 537–545.

Ueno, G., Hirose, R., Ida, K., Kumasaka, T. & Yamamoto, M. (2004). *J. Appl Cryst.* **37**, 867–873.

Vernede, X., Lavault, B., Ohana, J., Nurizzo, D., Joly, J., Jacquamet, L., Felisaz, F., Cipriani, F. & Bourgeois, D. (2006). *Acta Cryst.* D**62**, 253–261.

Zhang, Z., Sauter, N. K., van den Bedem, H., Snell, G. & Deacon, A. M. (2006). *J. Appl. Cryst.* **39**, 112–119.